TRR
JOURNAL OF THE TRANSPORTATION RESEARCH BOARD

Research Article

Transportation Research Record
1–12

DOI: 10.1177/0361198121991850
journals.sagepub.com/home/trr
SAGE

Simple Methodology for the Development and Analysis of Local Driving Cycles Applied in the Study of Cars and Motorcycles in Recife, Brazil

Guilherme Medeiros Soares de Andrade[1], Fernando Wesley Cavalcanti de Araújo[1], Maurício Pereira Magalhães de Novaes Santos[1], Silvio Jacks dos Anjos Garnés[2], and Fábio Santana Magnani[1]

Abstract

Standard driving cycles are usually used to compare vehicles from distinct regions, and local driving cycles reproduce more realistic conditions in specific regions. In this article, we employed a simple methodology for developing local driving cycles and subsequently performed a kinematic and energy analysis. As an application, we employed the methodology for cars and motorcycles in Recife, Brazil. The speed profile was collected using a smartphone (1 Hz) validated against a high precision global positioning system (10 Hz), presenting a mean absolute error of 3 km/h. The driving cycles were thus developed using the micro-trip method. The kinematic analysis indicated that motorcycles had a higher average speed and acceleration (32.5 km/h, 0.84 m/s^2) than cars (22.6 km/h, 0.55 m/s^2). As a result of the energy analysis, it was found that inertia is responsible for most of the fuel consumption for both cars (59%) and motorcycles (41%), but for motorcycles the aerodynamic drag is also relevant (36%). With regards to fuel consumption, it was found that the standard driving cycle used in Brazil (FTP-75; 2.47 MJ/km for cars and 0.84 MJ/km for motorcycles) adequately represents the driving profile for cars (2.46 MJ/km), and to a lesser extent motorcycles (0.91 MJ/km) in off-peak conditions. Finally, we evaluated the influence of the vehicle category on energy consumption, obtaining a maximum difference of 38% between a 2.0 L sports utility vehicle and a 1.0 L hatchback.

A driving cycle is a time-speed series used to represent the driving pattern of vehicles in real-world traffic. There are standard driving cycles (SDCs), used for nationwide comparisons, and local driving cycles (LDCs), that are important for regional analysis. These LDCs can be obtained by recording the real movement of a vehicle in traffic, followed by a constructing method that preserves their major kinematic parameters. In this study, we employed a simple methodology to register the speed profile of the vehicle using a smartphone, performed a kinematic characterization of the data set, developed LDCs using the micro-trip method, and finally conducted an energy analysis. The methodology was applied both for cars and motorcycles in Recife, a major Brazilian city.

Governments, research institutes, and manufacturers use SDCs in dynamometers to estimate fuel consumption in standardized testing (*1*). Since 2008, the United States has adopted the five-cycle method, consisting of the federal test procedure (FTP-75), which is performed in cold start and hot start, the highway fuel economy test cycle (HWFET), and the supplemental federal test procedures US06 and SC03 (*2*). The European Union finished the transition from the new European driving cycle (NEDC) to the worldwide harmonized light vehicles test cycles (WLTC) in January 2019 (*3*). The WLTC is a transient driving cycle and reflects real-world conditions better if compared to the stationary NEDC. In Brazil, the fuel economy is measured for cars and motorcycles using FTP-75 for city conditions and the HWFET for highway conditions (*4*). Despite all efforts to elaborate an SDC to estimate fuel consumption, there is increasing evidence

[1]Department of Mechanical Engineering, Universidade Federal de Pernambuco, Recife, Brazil
[2]Department of Cartographic Engineering, Universidade Federal de Pernambuco, Recife, Brazil

Corresponding Author:
Guilherme Medeiros Soares de Andrade,
guilherme.soaresandrade@ufpe.br

that the deviation from the results obtained in approval tests (SDCs) and real-world situations, can be as high as 60% (*5*). LDCs take into account the vehicle fleet, topography, and driver behavior, better representing the local conditions (*6–8*).

The most employed methods for collecting driving data consist of equipping the vehicles with a global positioning system (GPS) receiver to measure and record the vehicle speed. GPS recording frequencies for driving cycle development usually vary from 1 to 10 Hz. Several papers employed a recording frequency of 1 Hz, which was considered adequate to capture the vehicle dynamics (*1, 7, 9–16*). In addition to GPS receivers, smartphones can also provide the actual position and speed with a reasonable accuracy, and most of them offer an accelerometer, magnetometer, and gyroscope to improve the speed prediction. Rechkemmer et al. published a study evaluating the GPS information obtained from smartphones (*17*). According to them, the mean error between the speed obtained using a smartphone and test equipment is 0.87 m/s with a standard deviation of 0.28 m/s.

The set of speed data is then processed to develop a shorter driving cycle with the same kinematic characteristics. The micro-trip method is an established approach that is used to develop driving cycles (*18*). A micro-trip is defined as a trip segment in which the vehicle begins and ends at zero speed (*10*). During this time interval, the vehicle can perform any number of accelerations and decelerations (*8*). The first important DC constructed using micro-trips was the California Unified Cycle 1992 (LA-92), developed by the California Air Resources Board (CARB) (*19*). After extracting micro-trips from real-world data, they were combined and permuted until a representative driving cycle for Los Angeles, California was obtained. Over the years, several other cycles were developed. Micro-trips have been employed to generate driving cycles for motorcycles, passenger cars, and even trucks (*6, 9, 11, 20–25*). This method allows utilization of data collected from the car-chasing technic, directly from the vehicle studied, or obtained from a traffic simulator (*6, 9, 22–24*).

This study aims to develop real-world LDCs for cars and motorcycles, during off-peak hours, in Recife, Brazil. Additionally, we perform a kinematic and energy analysis of the cycles developed, comparing them to established SDCs. To achieve these objectives, we collected the speed data of the vehicle using a smartphone that was validated against a precise GPS receiver. Furthermore, we employed the micro-trip method to build the LDCs. We performed a kinematic analysis comparing both the LDCs and SDCs and an energy analysis for the local driving cycle (LDC) of the car and FTP-75, considering different categories and the engine displacement sizes of passenger cars.

Simple Methodology for Developing and Analyzing LDCs

In the development stage of an LDC, the authors usually follow three steps: route selection, speed-time data collection, and cycle construction. In turn, the analysis stage comprises the kinematic characterization, the simulation of the dynamics of the vehicle, and the energy consumption calculation.

Development Stage of an LDC. The selected testing route has to capture significant aspects of the city, such as the traffic profile, the topography, and the relevance of the roads for citizens. The most reliable way to collect the speed-time vector is from the on-board technique, in which the measuring device is present in the vehicle during the test (*18, 25*). The vehicle (motorcycle or car) must represent the fleet and the driver must have experience of the route. Usually, the speed evolution during the trip is captured using a GPS, which could be a specialized receiver (1 or 10 Hz) or a smartphone (1 Hz), the choice depends on costs, data quality, and availability. After collecting the raw data, there is a filtering stage to correct gross measurement errors, such as signal losses, false zero speeds, and unreal accelerations/decelerations (*1, 7, 10, 26*).

Driving cycles have different speed-time patterns. Their visual comparison is not straightforward, thus authors define their kinematic characteristic parameters (CPs) to compare them numerically (*18*). In this study, nine CPs are evaluated, as listed in Table 1.

The process of construction of a driving cycle employing the micro-trip method involves six steps, as follows (*11*): (1) combine all the measurements in a single-speed vector (all-trips vector); (2) obtain the kinematic parameters of the all-trips vector; (3) decompose the all-trips vector in micro-trips (stretches of the trip between two occurrences of zero speed); (4) combine the micro-trips randomly maintaining the resulting cycle time within a certain specific range (e.g., 10–40 min); (5) calculate the kinematic parameters of the combined vector; and (6) repeat from step 4 until the error between the CPs of the combined cycle and the all-trips vector is less than a certain specified threshold (according to Seedam et al., an LDC is equivalent to the all-trips vector if the average difference in their CPs values is under 4% [*22*]).

Vehicle Dynamics and Energy Model. To evaluate the dynamics of the vehicle, we employ Newton's Second Law considering its physical characteristics (Equation 1; [*27*]):

$$ma = F_{\text{wheel}} - mg\sin\theta - C_r mg\cos\theta - K_A V^2 \qquad (1)$$

Table 1. Characteristic Parameters Evaluated in this Study

Parameters	Symbol	Definition
Cycle duration	t (s)	Total time of the driving cycle
Average speed	V (km/h)	Average speed including zero speed
Average running speed	V_r (km/h)	Average speed excluding zero speed
Average acceleration	a (m/s^2)	Average acceleration rate above 0.0 m/s^2
Average deceleration	d (m/s^2)	Average deceleration rate below 0.0 m/s^2
Time spent idling	T_i (%)	Time proportion in which V =0.0 km/h and a = 0.0 m/s^2
Time spent accelerating	T_a (%)	Time proportion in which $a>$ 0.0 m/s^2
Time spent decelerating	T_d (%)	Time proportion in which $a<$ 0.0 m/s^2
Time spent cruising	T_c (%)	$100\% - T_i - T_a - T_d$
Speed standard deviation	σ_v (km/h)	Speed standard deviation for the entire driving cycle (km/h)

where the first term on the right-hand side of the equation is the force on the wheels (traction or braking), the second is the force of gravity (for which θ is the angle of inclination), $C_r mg\cos\theta$ is the rolling resistance (e.g., tire, spring, and damper deformation), and the fourth term, $K_A V^2$, is the aerodynamic drag. Also, $K_A = \frac{1}{2}\rho A C_D$, where ρ is the specific mass of the air, A is the frontal area of the vehicle, and C_D is the drag coefficient.

To calculate the energy consumption, it is necessary to perform either a dynamometer test or a computer simulation of the movement. In both strategies, information about the vehicle resistances is necessary. In Brazil, the official values for the resistance forces on vehicles during movement are obtained from the standard coast down test (*28*). Additionally, these values for passenger cars can be requested from the National Institute of Metrology, Standardization and Industrial Quality (INMETRO). This test is performed with the vehicle decelerating freely ($F_{\text{wheel}} = 0$) over a horizontal test track ($\theta = 0$), therefore Equation 1 is transformed into Equation 2:

$$ma_{\text{coastdown}} = -C_r mg - K_A V^2 \quad (2)$$

Figure 1 displays the speed profile of the coast down experiment ($a_{\text{coastdown}}$ can be easily obtained from the recorded $V_{\text{coastdown}}$). If the mass of the ensemble (vehicle, driver, and equipment) is known, Equation 2 can be adjusted to the experimental curve, yielding C_r (rolling coefficient) and K_A (aerodynamic drag factor) for the tested vehicle.

Considering a general movement again, Equation 1 can be multiplied by the speed, resulting in the power necessary on the wheels to provide the desired movement (Equation 3):

$$P_{\text{wheel}} = \left(ma + mg\sin\theta + C_r mg\cos\theta + K_A V^2\right)V \quad (3)$$

If P_{wheel} is positive this demands the activation of the engine by the throttle, and if P_{wheel} is negative this demands braking. P_{wheel} can be related to the maximum

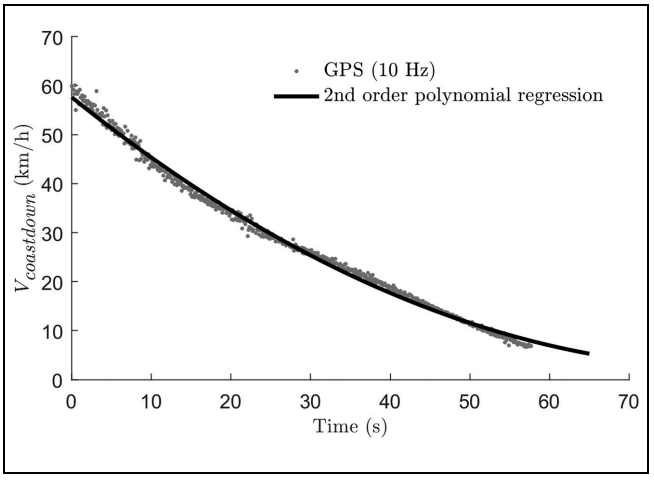

Figure 1. Speed evolution during a coast down testing pass.

power generated by the engine at a given engine speed ($P_{max,eng}$), requiring the transmission efficiency (η_t). This ratio is defined as the throttle usage (α), between 0 and 1, as described in Equation 4.

$$\alpha = P_{wheel} / \left(\eta_t P_{max,eng}\right) \quad (4)$$

To model the engine power curve, we used an empirical correlation developed by Ni and Henclewood, Equation 5 (*29*). In this equation, we limited the engine power curve between the minimum engine speed (Ω_{min}) and maximum engine speed (Ω_{min}). The relevant parameters of the engine are also needed: engine speed at peak torque ($\Omega_{peak,tor}$), engine speed at peak power ($\Omega_{peak,pow}$), and the peak power of the engine (P_{max}).

$$P_{max,eng}(\Omega) = \begin{cases} C_1\Omega_{min} + C_2\Omega_{min}\left(\Omega_{min} - \Omega_{peak,tor}\right)^2 & \Omega < \Omega_{min} \\ C_1\Omega + C_2\Omega\left(\Omega - \Omega_{peak,tor}\right)^2 & \Omega_{min} \leq \Omega \leq \Omega_{max} \\ 0 & \Omega > \Omega_{max} \end{cases} \quad (5)$$

where

$$C_1 = \frac{P_{\max}}{2\Omega_{\text{peak, pow}}{}^2}\left(3\Omega_{\text{peak, pow}} - \Omega_{\text{peak, tor}}\right)$$

$$C_2 = -\frac{P_{\max}}{2\Omega_{\text{peak, pow}}{}^2\left(\Omega_{\text{peak, pow}} - \Omega_{\text{peak, tor}}\right)}$$

Also, based on the power necessary on the wheels, we can evaluate the power of the burnt fuel (P_{fuel}), considering the transmission efficiency (η_t), the engine efficiency (η_{eng}), and assuming there is no fuel consumption on braking ($P_{\text{wheel}} < 0$). Even if the vehicle is stopped ($V = 0$ and $a = 0$), it is still consuming fuel (P_{idle}) to keep the engine running and to provide energy for the accessories (e.g., air conditioning, alternator), Equation 6.

$$P_{\text{fuel}} = \begin{cases} \frac{\max(P_{\text{wheel}}, 0)}{\eta_t \eta_{\text{eng}}} & \text{for} V \neq 0 \text{ or } a \neq 0 \\ P_{\text{idle}} & \text{for} V = 0 \text{ and } a = 0 \end{cases} \quad (6)$$

An empirical correlation was used to model the efficiency of the engine (Equation 7), provided by Ben-Chaim et al. (*30*). The energy efficiency of the engine (η_{eng}) is the function of three parameters: the maximum efficiency of the engine (η_0), corrected by factors (μ_{rev}) that consider the engine speed (Ω), and (μ_{pow}) that consider the throttle usage (α).

$$\eta_{eng}(\Omega, \alpha) = \eta_0 \mu_{rev}(\Omega)\mu_{pow}(\alpha) \quad (7)$$

where

$$\mu_{rev}(\Omega) = 0.7107 + 0.9963\left(\frac{\Omega}{\Omega_{\text{peak, pow}}}\right) - 1.0582\left(\frac{\Omega}{\Omega_{\text{peak, pow}}}\right)^2 + 0.3124\left(\frac{\Omega}{\Omega_{\text{peak, pow}}}\right)^3$$

$$\mu_{pow}(\alpha) = 0.234 + 1.0592\alpha + 0.8149\alpha^2 - 1.2121\alpha^3$$

The maximum efficiency of the engine (η_0) is an input that should be informed by the researcher in Equation 7. In this study, to obtain the η_0 of the vehicle we performed a two-step analysis: (1) we measured the fuel consumption of the vehicle in a known trajectory (e.g., SDC, LDC, floating-data), and (2) in possession of the real fuel consumption, of the trajectory, and of the vehicle data, we simulated the vehicle fuel consumption varying η_0 until the consumption obtained in the simulation was similar to the consumption obtained in the real test. As can be seen in the previous expressions, the engine speed is an important parameter, therefore we need to consider the drivetrain system. In this study, we used the real gear ratio of the simulated vehicles. The gears are shifted up if the engine speed is above 2,200 rpm and shifted down if the engine speed is below 1,100 rpm.

The mechanical energy on the wheels (E_{wheel}) to overcome the resistances is the integral of P_{wheel} throughout the cycle (Equation 8):

$$E_{\text{wheel}} = \frac{1}{L}\int P_{\text{wheel}} dt \quad (8)$$

Similarly, in Equation 9, the total fuel energy (E_{fuel}) is the integral of the fuel power (P_{fuel}). In both equations, L is the total distance of the driving cycle.

$$E_{\text{fuel}} = \frac{1}{L}\int P_{\text{fuel}} dt \quad (9)$$

Both energies on the wheel (Equation 10) and contained in the fuel (Equation 11) can be split according to the various resistances to movement: inertia (ine), gravity (grav), rolling (rol), drag (aero), and idling (idle), in which the subscripts 'w' and 'f' indicate wheel and fuel, respectively. Thus:

$$E_{\text{wheel}} = E_{\text{w, ine}} + E_{\text{w, grav}} + E_{\text{w, rol}} + E_{\text{w, aero}} \quad (10)$$

$$E_{\text{fuel}} = E_{\text{f, ine}} + E_{\text{f, grav}} + E_{\text{f, rol}} + E_{\text{f, aero}} + E_{\text{f, idle}} \quad (11)$$

Case Study: Recife, Brazil

Recife is a major Brazilian city, located in the Northeastern Region (Figure 2). The city is one of the oldest in the Americas (founded in 1537), and is an important economic, tourist, and medical center in the region. It has 1.6 million inhabitants, with approximately 400 thousand passenger cars and 150 thousand motorcycles (the complete metropolitan region has 4.1 million people) (*31*).

To perform the experiments in this study, we employed a pair of geodetic receivers Topcon Hiper Lite + , capable of receiving a satellite signal up to 10 Hz. We also employed a smartphone (Asus Zenfone 4) equipped with a gyroscope, accelerometer, and compass to collect the data at 1 Hz. The planimetric precision of a smartphone is usually between 1 and 4 m, whereas in the geodetic receiver the precision is more accurate: 1.5 cm. For altimetric measurements, the results are not accurate for the smartphone equipment, and the error can achieve dozens of meters.

We chose a 17.1 km trajectory comprising three of the major arterial roads in the city (Recife Avenue, Abdias de Carvalho Avenue, and Mascarenhas de Moraes Avenue; Figure 2). This trip length is very similar to FTP-75 (17.7 km). The tests with cars (Fiat Argo 1.3L, Hyundai HB20 1.0 L, VW Golf 1.0 L) and motorcycles (Honda CB 300 and Honda CG 125) were performed during the afternoon in off-peak hours (14–17 h), from November 2018 to October 2019 on weekdays,

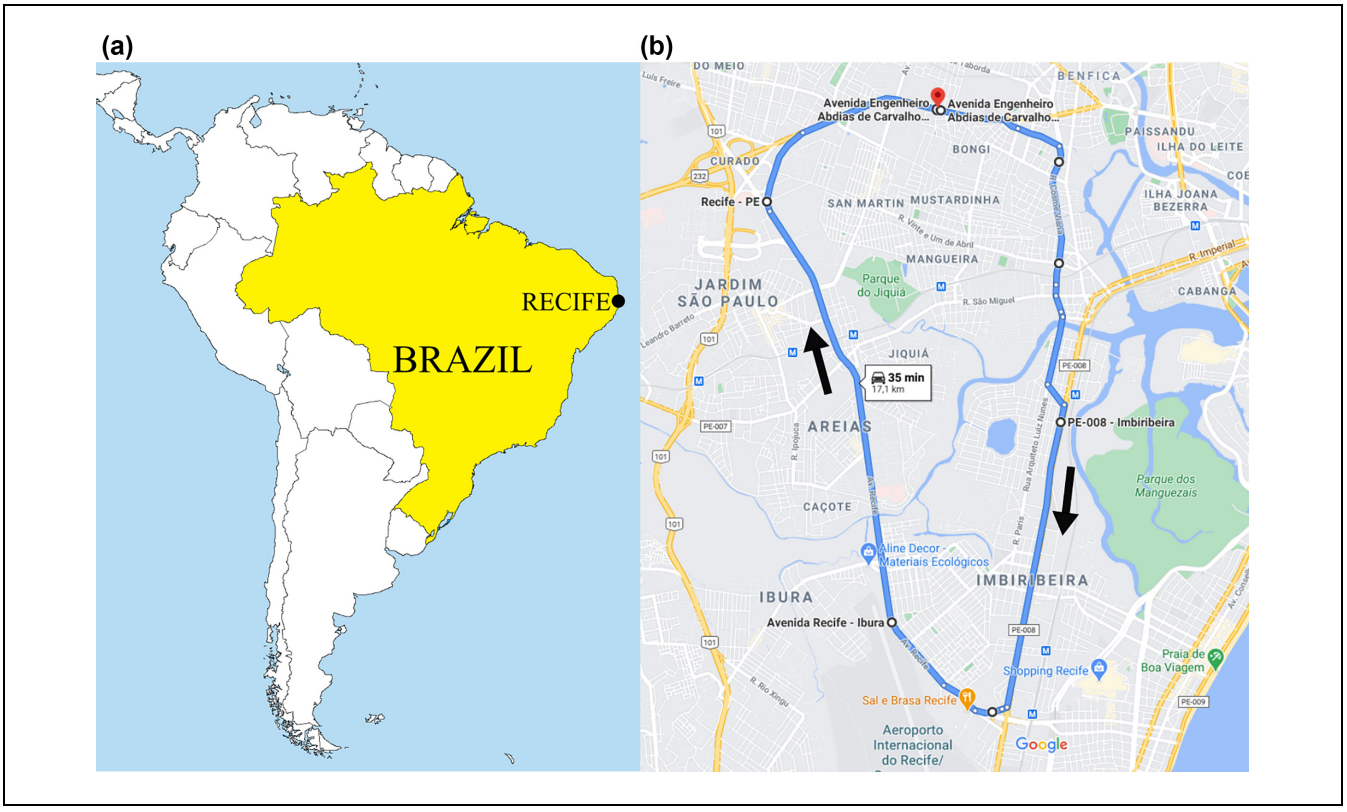

Figure 2. (*a*) Location of Recife in Brazil and (*b*) test route for passenger cars and motorcycles in Recife, Brazil (Source: Google Maps®).

Table 2. Engine and Vehicle Parameters Used for the Energy Simulation

	Parameter	Car	Motorcycle
η_0	Maximum engine efficiency	20%	19%
m	Total mass (vehicle + pilot[1])	1126 kg	280 kg
C_r	Rolling resistance coefficient	0.010	0.015
K_A	Aerodynamic drag factor	0.486 N/(m/s)^2	0.37 N/(m/s)^2

[1]The pilot and the testing equipment weigh 136 kg, according to Brazilian Law ABNT 6601.

comprising all seasons. According to the GPS receiver, in the trajectory selected the average slope was 0.4% (also, the elevation in the route is 6 m ± 4 m). Therefore, in this study we considered the slope negligible. This result is in accordance with the records from the official city report, in which the road slope is between 0% and 3.3% for the largest part of the road network, contributing to the assumption that Recife has a flat topography (*32*).

The parameters of the simulated vehicles are listed in Table 2. The car simulated represents a reference vehicle (a vehicle with average parameters from the most sold category in Brazil: a hatchback with manual transmission and a 1.0 L engine), and the motorcycle simulated was a Honda CB 300 (a medium-sized motorcycle with manual transmission and a 300 cc engine), one of the models most sold in Brazil in its category (*33*). The values of C_r and K_A for the car were obtained from INMETRO (*34*). For the motorcycle, K_A and C_r were obtained from the coast down experiment (Equation 2 and Figure 1), because there are not official public records for the coefficient of motorcycles in Brazil. The coast down was validated after performing a test for a passenger car with known parameters. On comparing the parameters obtained from the test with the official values, we found an error of 12%, which we considered acceptable. The maximum engine efficiency (η_0) was defined to result in the same consumption of FTP-75 for a car, and the Recife floating data for motorcycles (*34*).

To develop the LDCs, we obtained 405 micro-trips for passenger cars and 350 micro-trips for motorcycles. For the sake of comparison, Arun et al. collected 236

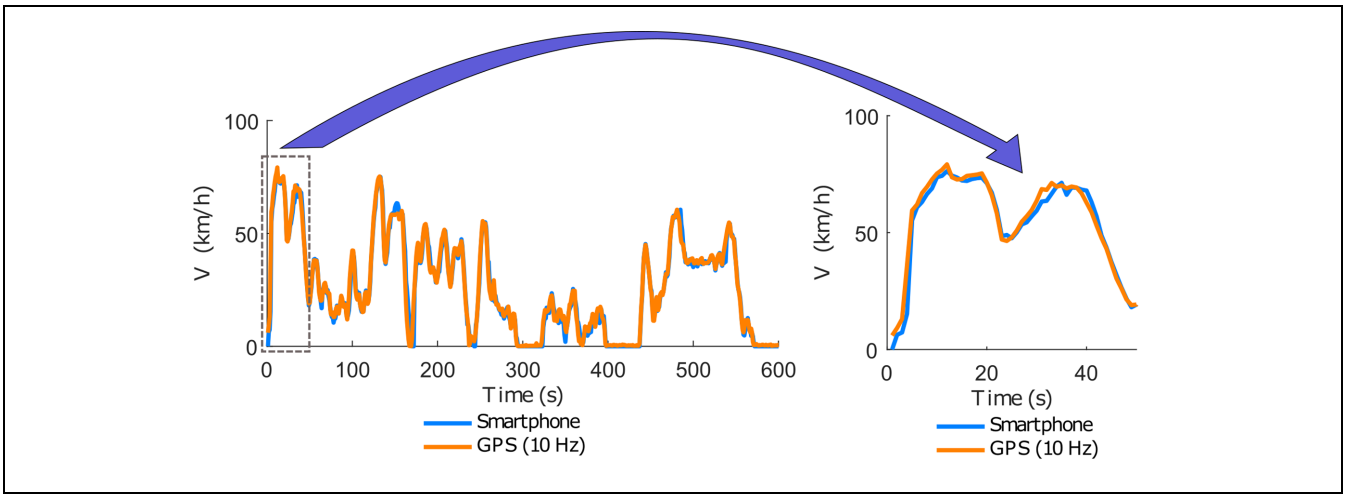

Figure 3. Comparison between the speed data recorded with the smartphone (1 Hz) and GPS (10 Hz).

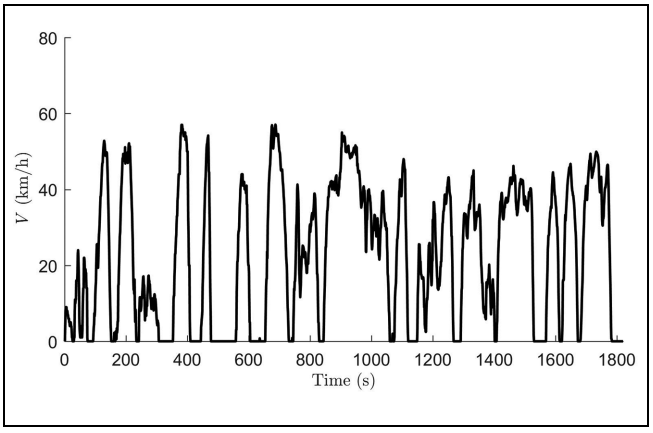

Figure 4. Recife driving cycle for passenger cars.

micro-trips for cars and 269 for motorcycles for the same off-peak condition (*11*). Pouresmaeili et al. obtained 273 micro-trips in their study of Mashhad (Iran) and Yang et al. obtained 373 micro-trips for Nanjing (China), for both peak and off-peak conditions (*10, 25*).

On the first test day, we used both the GPS receiver (Topcon Hiper Lite, 10 Hz) and the smartphone (Asus Zenfone 4,1 Hz) simultaneously to verify if both would present similar results for the same route. After comparing the results, we found a mean average error of 3.0 km/h between the two devices. This difference is considered adequate in the Brazilian norm for chassis dynamometer testing (*4*). Figure 3 provides part of the data collection for the GPS (10 Hz) and the smartphone (1 Hz).

The representativeness of the data collected for Recife traffic conditions was checked using Google Maps®. Google Maps® does not provide the instantaneous speed of the road; however, it presents the average speed and the expected travel time, considering the real-time traffic conditions. We monitored and registered the traffic conditions every 5 min during the tests. The results indicated that the passenger cars tested on the road showed a similar behavior in traffic in comparison with the average speed given by the tool at the same time interval (average difference of 5% for passenger cars). From the small difference between the average speed obtained by the driver and the tool, we imply that the driver followed the expected traffic behavior. For motorcycles, the same analysis provided a higher difference considering the speed (24%), this is explained by Google Maps® only presenting the travel time and average speed for cars during the period of the tests.

Results and Analysis

Using the method of cycle development presented in the methodology, the 755 micro-trips (405 for cars and 350 for motorcycles) recorded during the experiments on the Recife avenues generated the LDCs presented in Figure 4 (cars) and Figure 5 (motorcycles). The cycle developed for cars, called Recife car driving cycle (RCDC), has a duration of 1,820 s (30 min and 20 s) traveling 11.4 km. The developed Recife motorcycle driving cycle (RMDC) has a duration of 2,106 s (35 min and 6 s), for a 19.0 km trip. Both cycles present a duration between 10 and 40 min, described as the lower and upper timing limits recommended according to literature (*11*).

The developed driving cycle presents similar CPs (with the difference under the specified threshold of 4%) and has a shorter duration if compared to the original all-trips vector. The comparison between the obtained driving cycles and the original all-trips vectors is summarized in Table 3.

The motorcycles cycle, RMDC (Figure 5), presents a higher number of accelerations and decelerations than

Table 3. Characteristic Parameters for the RCDC, RMDC, and the Respective Original All-Trips Vectors

Driving cycle	t (s)	L (km)	V (km/h)	V_r (km/h)	a (m/s^2)	d (m/s^2)	T_c	T_i	T_a	T_d	σ_v (km/h)
RMDC	2,106	19.0	32.5	38.4	0.76	–0.80	2%	15%	43%	41%	21.5
All-trips of motorcycles	25,805	240.0	33.5	39.2	0.72	–0.79	2%	15%	44%	40%	21.7
RCDC	1,820	11.4	22.6	29.6	0.48	–0.56	5%	24%	38%	33%	18.4
All-trips of cars	33,352	222.7	24.0	31.4	0.46	–0.52	6%	23%	37%	33%	18.7

Note: RCDC = Recife driving cycle for passenger cars; RMDC = Recife driving cycle for motorcycles.

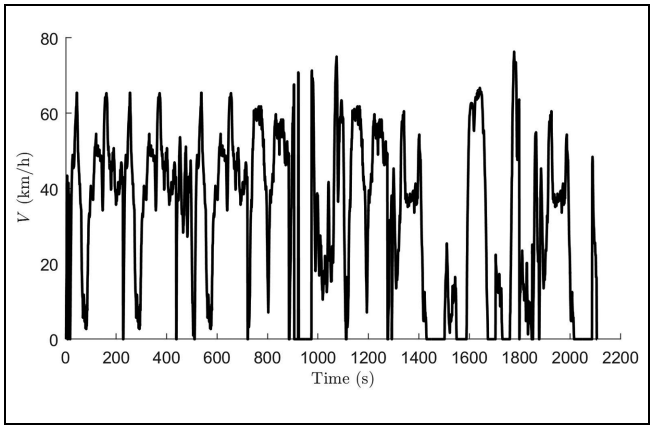

Figure 5. Recife driving cycle for motorcycles.

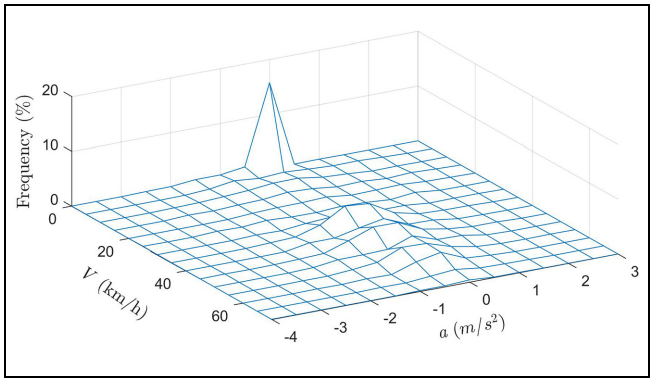

Figure 6. Speed acceleration frequency distribution for motorcycles.

the cars cycle, RCDC (Figure 4). It also presents higher values for the average acceleration, average speed, average running speed, and average deceleration (in absolute values) when compared to cars (Table 3). The duration difference between the RMDC and the RCDC is approximately 10%, and the distance difference is 66%. Those values reveal that cars require a longer time to move in Recife and this reflects the notable ability of motorcycles to filter through traffic at low speed to move as fast as possible.

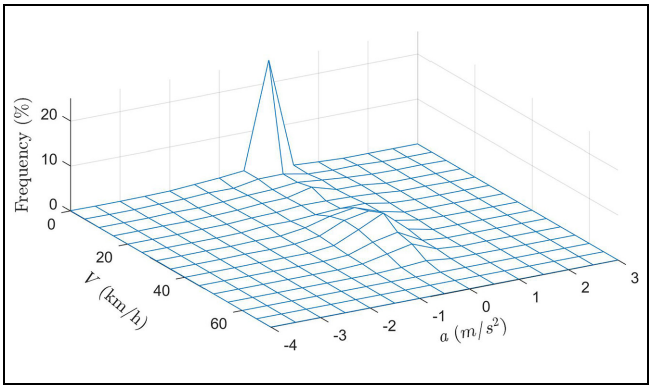

Figure 7. Speed acceleration frequency distribution for passenger cars.

The speed-acceleration frequency distribution of the Recife driving cycles for motorcycles and cars are displayed in Figures 6 and 7. It can be observed that motorcycles have a higher occurrence of non-null speed between 30 and 60 km/h (57%) and that 55% of non-null speeds for cars occur between 25 and 55 km/h.

Table 4 compares the CPs of the obtained RMDC, FTP-75 (used in Brazil and the USA), and the world motorcycle test cycle (WMTC). The RMDC presented an average speed similar to FTP-75 (5% lower), but higher average accelerations (49% higher) and decelerations (38% higher), providing more aggressive behavior in traffic. In comparison to the WMTC, the RMDC has a higher acceleration (95% higher) and lower average speed (44% lower).

For passenger cars (Table 5), there is a relevant difference in the average speed for the RCDC in comparison with FTP-75 (34% lower), but a similar average acceleration (4% lower) and average deceleration (3% lower). In comparison to the WLTC, the RCDC has a lower average speed (51% lower), and a higher average acceleration, and deceleration (20% and 24%, respectively).

The RCDC can also be compared to cycles for other Brazilian cities: Fortaleza and Santa Maria (*35, 36*). Recife and Fortaleza have similar average speeds in their driving cycles (the speed in Recife is 6% lower, Table 5). Both cities are the capital of their states and are located

Table 4. Kinematic Characteristic Parameters for the RMDC

Driving cycle	t (s)	L (km)	V (km/h)	V_r (km/h)	a (m/s^2)	d (m/s^2)	T_c	T_i	T_a	T_d	σ_v (km/h)
RMDC	2106	19.0	32.5	38.4	0.76	–0.80	2%	15%	43%	41%	21.5
FTP-75	1874	17.7	34.1	41.6	0.51	–0.58	8%	18%	39%	35%	25.7
WMTC	1800	28.9	57.8	63.4	0.39	–0.49	16%	9%	41%	34%	37.9

Note: RMDC = Recife driving cycle for motorcycles; FTP-75 = federal test procedure; WMTC = world motorcycle test cycle.

Table 5. Kinematic Characteristic Parameters for the RCDC

Driving cycle	t (s)	L (km)	V (km/h)	V_r (km/h)	a (m/s^2)	d (m/s^2)	T_c	T_i	T_a	T_d	σ_v (km/h)
RCDC	1820	11.4	22.6	29.6	0.48	–0.56	5%	24%	38%	33%	18.4
Fortaleza	1216	8.4	23.8	NA	NA	NA	0%	43%	30%	27%	NA
Santa Maria 5.p.m.	2017	11.7	30.8	NA	NA	NA	2%	NA	51%	48%	NA
FTP-75	1874	17.7	34.1	41.6	0.51	–0.58	8%	18%	39%	35%	25.7
WLTC	1800	23.3	46.5	53.2	0.41	–0.45	13%	4%	44%	40%	NA

Note: RCDC = Recife driving cycle for passenger cars; FTP-75 = federal test procedure; WLTC = worldwide harmonized light vehicles test cycles; NA = not available.

Table 6. Simulated Energy Parameters ($\boldsymbol{E}_{\text{wheel}}$ and $\boldsymbol{E}_{\text{fuel}}$) for the LDC and SDCs for a Motorcycle (Honda CB 300)

Driving cycle	E_{wheel} (MJ/km)	E_{fuel} (MJ/km)	$E_{\text{f, ine}}$ (MJ/km)	$E_{\text{f, rol}}$ (MJ/km)	$E_{\text{f, aero}}$ (MJ/km)	$E_{\text{f, idle}}$ (MJ/km)
RMDC	0.185	0.909	0.373 (41%)	0.180 (20%)	0.330 (36%)	0.027 (3%)
FTP-75	0.166	0.840	0.169 (20%)	0.171 (20%)	0.449 (53%)	0.051 (6%)
WMTC	0.284	1.992	0.442 (22%)	0.418 (21%)	1.086 (55%)	0.045 (2%)

Note: RMDC = Recife driving cycle for motorcycles; FTP-75 = federal test procedure; WMTC = world motorcycle test cycle.

in northeastern Brazil. For the sake of comparison, Fortaleza has 2.6 million inhabitants, 592 thousand cars and 298 thousand motorcycles (*31*). Santa Maria (0.26 million inhabitants, 100 thousand cars and 26 thousand motorcycles) is a smaller city in the Brazilian southern region and presents different traffic conditions if compared to Recife and Fortaleza. This feature can explain the difference in the average speed of Recife and Fortaleza in relation to Santa Maria (Recife has speed that is 27% lower). Table 5 also summarizes the splitting of the time spent accelerating, decelerating, idling, and cruising. The Brazilian cities notably have a lower cruising time when compared to the SDCs (WLTC and FTP-75). Also, the RCDC and Fortaleza present a higher idling time when compared to both standard cycles.

Table 6 summarizes the splitting of the fuel consumption of the motorcycle in inertia, rolling resistance, aerodynamic drag, and idling (Equation 11); considering RMDC, FTP-75, and WMTC. The RMDC has a lower energy consumption to overcome the aerodynamic drag (0.330 MJ/km) compared to FTP-75 (0.449 MJ/km) owing to its lower average speed, and has a higher energy consumption to overcome inertia (0.373 MJ/km) because of its higher acceleration. The WMTC has higher values of energy consumption caused by the higher average speed (V multiplies all the terms in Equation 3), evidenced by the higher percentage of drag (55%).

Table 7 lists the results for cars. It is noticeable how the RCDC has a lower energy consumption to overcome aerodynamic drag (because of its lower average speed). In relation to inertia, the consumption of RCDC is closer to FTP-75 (–0.227 MJ/km) than WLTC (–0.441 MJ/km), because of the similar average acceleration and time spent accelerating between RCDC and FTP-75. The energy consumption for aerodynamic drag in the RCDC is much lower than both the FTP-75 and WLTC. We propose that this happens because of the RCDC lower average speed and higher time spent idling, reflected in the idling energy among the cycles.

Next, we studied how much energy is necessary to overcome the resistances (E_{wheel}) in the RCDC and FTP-75 using other usual car categories (Hatchback, Sedan, and SUV) in Brazil. To represent the other car categories, we employed an average vehicle for each category. This vehicle considered the average parameters of m, C_r, and K_A of all vehicles in the studied car category,

Table 7. Simulated Energy Parameters (E_{wheel} and E_{fuel}) for the Local Driving Cycles and Standard Driving Cycles for a Passenger Car (1.0 Hatchback)

Driving cycle	E_{wheel} (MJ/km)	E_{fuel} (MJ/km)	$E_{f,ine}$ (MJ/km)	$E_{f,rol}$ (MJ/km)	$E_{f,aero}$ (MJ/km)	$E_{f,idle}$ (MJ/km)
RCDC	0.358	2.457	1.438 (59%)	0.498 (20%)	0.246 (10%)	0.275 (11%)
FTP-75	0.383	2.469	1.211 (49%)	0.524 (21%)	0.603 (24%)	0.131 (5%)
WLTC	0.465	2.800	0.997 (36%)	0.700 (25%)	1.051 (38%)	0.051 (2%)

Note: RCDC = Recife driving cycle for passenger cars; FTP-75 = federal test procedure; WLTC = worldwide harmonized light vehicles test cycles.

Table 8. Mechanical Energy on the Wheels (E_{wheel}, MJ/km) for Representative Cars of the Brazilian Fleet

	Vehicle characteristics			FTP-75				RCDC			
Vehicle category and engine size	m	C_r	K_A	E_{wheel}	$E_{w,ine}$	$E_{w,rol}$	$E_{w,aero}$	E_{wheel}	$E_{w,ine}$	$E_{w,rol}$	$E_{w,aero}$
1.0 L Hatchback	1126	0.010	0.486	0.383	0.186	0.089	0.108	0.358	0.238	0.078	0.042
1.0 L Sedan	1138	0.011	0.520	0.398	0.187	0.096	0.116	0.369	0.239	0.084	0.045
1.6 L Hatchback	1229	0.012	0.505	0.424	0.202	0.110	0.113	0.399	0.258	0.098	0.044
1.6 L Sedan	1289	0.011	0.473	0.431	0.213	0.113	0.105	0.412	0.272	0.099	0.041
1.6 L SUV	1321	0.011	0.464	0.428	0.220	0.106	0.102	0.413	0.280	0.093	0.040
2.0 L Hatchback	1322	0.011	0.526	0.450	0.218	0.115	0.117	0.426	0.278	0.102	0.046
2.0 L Sedan	1460	0.009	0.500	0.456	0.246	0.101	0.109	0.443	0.311	0.089	0.042
2.0 L SUV	1477	0.010	0.778	0.529	0.242	0.114	0.173	0.478	0.310	0.100	0.068

Note: RCDC = Recife driving cycle for passenger cars; FTP-75 = federal test procedure; SUV = sports utility vehicle.

as informed by INMETRO (*34*). In Table 8, the mass increases progressively, C_r (associated with the rolling resistance, Equation 2) presents only a minor variation, and K_A (associated with the aerodynamic drag resistance, Equation 1) is clearly different for the SUV 2.0 L. In this analysis, we only consider the energy that the wheels should receive to perform the desired movement demanded by the studied cycle. Therefore, the engine is not accounted for in this analysis.

In Brazil, the vehicles are officially evaluated in urban conditions considering the standard driving cycle FTP-75 (*4*). In the FTP-75 (Table 8), most of the energy is spent on overcoming the inertia, usually by the aerodynamic and rolling resistance. In the RCDC, the inertia is also mainly responsible for the energy consumption. In second place is the rolling resistance, which is almost double the energy needed to overcome the aerodynamic drag. Additionally, the inertia resistance is higher in absolute and relative terms in the RCDC than the FTP-75. Also, the aerodynamic drag in the RCDC is not as relevant as it is in the FTP-75, as the maximum speed is higher than that achieved in the local driving cycle. It is possible to see from Table 8 how the energy demanded on the wheel is associated with the inertia is always higher for the same vehicle category in the RCDC if compared to the FTP-75, because of the higher acceleration. A similar case occurs for the energy needed to overcome the aerodynamic drag, which is always lower in the RCDC if compared to the FTP-75, because of the lower average speed.

If the categories are evaluated, it can be verified that the energy consumption increases as the engine displacement increases. As expected (from Equation 1), the main cause for increasing the energy demanded in the wheel is the inertia (because of the mass increment), followed by the rolling resistance (C_r is similar, but the mass also affects the energy demanded), and the aerodynamic drag (the variation is smaller because the vehicles do not present high variation in K_A, except for sports utility vehicles [SUVs]).

Evaluating the extreme cases in Table 8, comparing the last line (SUV 2.0 L) with the first (hatchback 1.0 L), for the FTP-75 driving cycle there is an increase of 38% in the E_{wheel}, constituted by an increase of 30% in $E_{w,ine}$, 28% in $E_{w,rol}$, and 60% in $E_{w,aero}$. Performing the same analysis for RCDC, the increases are 34% in the E_{wheel}, constituted by an increase of 30% in $E_{w,ine}$, 28% in $E_{w,rol}$, and 62% in $E_{w,aero}$.

Conclusion

In this study, we traveled 240 km by motorcycle and 223 km by car through the city of Recife during off-peak hours, registering the speed and position using a smartphone. Those vectors were divided into 755 micro-trips (350 for motorcycles and 405 for cars), which were recombined to build a reduced cycle for motorcycles (19 km, 2106 s), called the RMDC, and another for cars (11.4 km, 1820 s), called the RCDC.

The smartphone (1 Hz) record was validated against a 10 Hz GPS presenting an average error of 3 km/h. The resistance parameters (C_r and K_A) for cars were obtained from the literature and for motorcycles from the coast down experiment. The two driving cycles were then analyzed kinematically (e.g., average speed, acceleration, and idling time). A computer simulation was carried out, allowing an energy analysis of the cycles to be performed as well, splitting the total consumption into the aerodynamic, inertial, and rolling resistance, as well as the consumption during idling.

In possession of the results, we made several analyses. First, as expected, the motorcycle (average speed 33 km/h) is faster than the car (average speed 23 km/h), which can be explained by its ability to filter traffic. The motorcycles also have greater acceleration, owing to their smaller mass (combined mass in the test was 280 kg) compared to the car (combined mass in the test was 1126 kg). Also as expected, when comparing both motorcycles and passenger car driving cycles for Recife, motorcycles presented a 43% higher speed, 53% higher acceleration, and 46% higher deceleration on comparison with cars.

In the next step, we compared the cycles in Recife with the standard FTP-75 cycle (used for cars and motorcycles in the USA and Brazil), the WMTC (used for motorcycles in Europe), and the WLTC (used for cars in Europe). The RMDC (motorcycles in Recife) presented an average speed similar to the FTP-75, but greater acceleration, which made the energy consumption of the RMDC higher. As for the WMTC, the RMDC had a lower average speed, which caused a reduced energy consumption. The RCDC (cars in Recife) presented a lower average speed, but acceleration similar to FTP-75, resulting in a similar energy consumption. We also compared the RCDC with local cycles carried out in two other Brazilian cities. The average speed of Recife and Fortaleza (big cities) were similar, and the average speed of Santa Maria (medium-sized city) was higher. Then, in the last study presented in this paper, we simulated both the FTP-75 and RCDC using representative cars from the Brazilian fleet. The result was a variation of up to 38% in energy consumption comparing 1.0 L hatchback cars and 2.0 L SUVs.

As a main conclusion we emphasize the necessity to develop distinct cycles for motorcycles and for passenger cars. In addition, we found it is reasonable to employ smartphones to collect the speed data, provided they have been previously validated, considering a myriad of available smartphones exist in the market. Finally, in some cases FTP-75 can be employed to represent the local traffic behavior, as for cars in Recife in off-peak conditions, although the same conclusion could not be applied to motorcycles.

Acknowledgments

The authors would like to thank CAPES (Coordenação de Aperfeiçoamento de Pessoal do Ensino Superior) for financial support, to Reginaldo Andrade for collaborating in the driving and riding tests, and to CTTU for traffic data sharing.

Author Contributions

The authors confirm contribution to the paper as follows: study conception and design: Guilherme Andrade, Fábio Magnani; data collection: Guilherme Andrade, Fernando Araújo, Maurício Santos, Silvio Garnés, Fábio Magnani; analysis and interpretation of results: Guilherme Andrade, Fernando Araújo, Fábio Magnani; draft manuscript preparation: Guilherme Andrade, Fernando Araújo, Maurício Santos, Fábio Magnani. All authors reviewed the results and approved the final version of the manuscript.

Declaration of Conflicting Interests

The author(s) declared no potential conflicts of interest with respect to the research, authorship, and/or publication of this article.

Funding

The author(s) disclosed receipt of the following financial support for the research, authorship, and/or publication of this article: This study was financed by the Coordenação de Aperfeiçoamento de Pessoal de Nível Superior-Brasil (CAPES).

References

1. Wang, Z., J. Zhang, P. Liu, C. Qu, and X. Li. Driving Cycle Construction for Electric Vehicles Based on Markov Chain and Monte Carlo Method: A Case Study in Beijing. *Energy Procedia*, Vol. 158, 2019, pp. 2494–2499. https://doi.org/10.1016/j.egypro.2019.01.389.
2. EPA. *Vehicle and Fuel Emissions Testing*. U.S. Environmental Protection Agency.
3. Kühlwein, J., J. German, and A. Bandivadekar. Development of Test Cycle Conversion Factors Among Worldwide Light-Duty Vehicle CO2 Emission Standards. *The International Council on Clean Transportation*, Vol. 22, 2014, pp. 1–68. https://doi.org/http://www.theicct.org/sites/default/files/publications/ICCT_LDV-test-cycle-conversion-factors_sept2014.pdf.
4. ABNT NBR 7024. *Veículos Rodoviários Automotores Leves - Medição Do Consumo de Combustível - Método de Ensaio*. Normas, 2017.
5. Fontaras, G., N.-G. Zacharof, and B. Ciuffo. Fuel Consumption and CO2 Emissions from Passenger Cars in Europe – Laboratory Versus Real-World Emissions. *Progress in Energy and Combustion Science*, Vol. 60, 2017, pp. 97–131. https://doi.org/10.1016/j.pecs.2016.12.004.
6. Hung, W. T., H. Y. Tong, C. P. Lee, K. Ha, and L. Y. Pao. Development of a Practical Driving Cycle Construction Methodology: A Case Study in Hong Kong. *Transportation Research Part D: Transport and Environment*,

Vol. 12, No. 2, 2007, pp. 115–128. https://doi.org/10.1016/j.trd.2007.01.002.
7. Ma, R., X. He, Y. Zheng, B. Zhou, S. Lu, and Y. Wu. Real-World Driving Cycles and Energy Consumption Informed by Large-Sized Vehicle Trajectory Data. *Journal of Cleaner Production*, Vol. 223, 2019, pp. 564–574. https://doi.org/10.1016/j.jclepro.2019.03.002.
8. Mayakuntla, S. K., and A. Verma. A Novel Methodology for Construction of Driving Cycles for Indian Cities. *Transportation Research Part D: Transport and Environment*, Vol. 65, 2018, pp. 725–735. https://doi.org/10.1016/j.trd.2018.10.013.
9. Amirjamshidi, G., and M. J. Roorda. Development of Simulated Driving Cycles for Light, Medium, and Heavy Duty Trucks: Case of the Toronto Waterfront Area. *Transportation Research Part D: Transport and Environment*, Vol. 34, 2015, pp. 255–266. https://doi.org/10.1016/j.trd.2014.11.010.
10. Pouresmaeili, M. A., I. Aghayan, and S. A. Taghizadeh. Development of Mashhad Driving Cycle for Passenger Car to Model Vehicle Exhaust Emissions Calibrated Using On-Board Measurements. *Sustainable Cities and Society*, Vol. 36, 2018, pp. 12–20. https://doi.org/10.1016/j.scs.2017.09.034.
11. Arun, N. H., S. Mahesh, G. Ramadurai, and S. M. S. Nagendra. Development of Driving Cycles for Passenger Cars and Motorcycles in Chennai, India. *Sustainable Cities and Society*, Vol. 32, 2017, pp. 508–512. https://doi.org/10.1016/j.scs.2017.05.001.
12. Wang, Q., H. Huo, K. He, Z. Yao, and Q. Zhang. Characterization of Vehicle Driving Patterns and Development of Driving Cycles in Chinese Cities. *Transportation Research Part D: Transport and Environment*, Vol. 13, No. 5, 2008, pp. 289–297. https://doi.org/10.1016/j.trd.2008.03.003.
13. Lai, J., L. Yu, G. Song, P. Guo, and X. Chen. Development of City-Specific Driving Cycles for Transit Buses Based on VSP Distributions: Case of Beijing. *Journal of Transportation Engineering*, Vol. 139, No. 7, 2013, pp. 749–757. https://doi.org/10.1061/(asce)te.1943-5436.0000547.
14. Knez, M., T. Muneer, B. Jereb, and K. Cullinane. The Estimation of a Driving Cycle for Celje and a Comparison to Other European Cities. *Sustainable Cities and Society*, Vol. 11, 2014, pp. 56–60. https://doi.org/10.1016/j.scs.2013.11.010.
15. Esteves-Booth, A., T. Muneer, H. Kirby, J. Kubie, and J. Hunter. The Measurement of Vehicular Driving Cycle Within the City of Edinburgh. *Transportation Research Part D: Transport and Environment*, Vol. 6, No. 3, 2001, pp. 209–220. https://doi.org/10.1016/S1361-9209(00)00024-9.
16. Pathak, S. K., V. Sood, Y. Singh, and S. A. Channiwala. Real World Vehicle Emissions: Their Correlation with Driving Parameters. *Transportation Research Part D: Transport and Environment*, Vol. 44, 2016, pp. 157–176. https://doi.org/10.1016/j.trd.2016.02.001.
17. Rechkemmer, S. K., X. Zang, A. Boronka, W. Zhang, and O. Sawodny. Utilization of Smartphone Data for Driving Cycle Synthesis Based on Electric Two-Wheelers in Shanghai. *IEEE Transactions on Intelligent Transportation Systems*, Vol. PP, No. 99, 2019, pp. 1–11. https://doi.org/10.1109/TITS.2019.2961179.
18. Huertas, J. I., L. F. Quirama, M. Giraldo, and J. Díaz. Comparison of Three Methods for Constructing Real Driving Cycles. *Energies*, Vol. 12, No. 4, 2019, P. 665. https://doi.org/10.3390/en12040665.
19. Giakoumis, E. G. *Driving and Engine Cycles*. Springer, Cham, 2016.
20. Tsai, J. H., H. L. Chiang, Y. C. Hsu, B. J. Peng, and R. F. Hung. Development of a Local Real World Driving Cycle for Motorcycles for Emission Factor Measurements. *Atmospheric Environment*, Vol. 39, No. 35, 2005, pp. 6631–6641. https://doi.org/10.1016/j.atmosenv.2005.07.040.
21. Tong, H. Y., H. D. Tung, W. T. Hung, and H. V. Nguyen. Development of Driving Cycles for Motorcycles and Light-Duty Vehicles in Vietnam. *Atmospheric Environment*, Vol. 45, No. 29, 2011, pp. 5191–5199. https://doi.org/10.1016/j.atmosenv.2011.06.023.
22. Seedam, A., T. Satiennam, T. Radpukdee, and W. Satiennam. Development of an Onboard System to Measure the On-Road Driving Pattern for Developing Motorcycle Driving Cycle in Khon Kaen City, Thailand. *IATSS Research*, Vol. 39, No. 1, 2015, pp. 79–85. https://doi.org/10.1016/j.iatssr.2015.05.003.
23. Koossalapeerom, T., T. Satiennam, W. Satiennam, W. Leelapatra, A. Seedam, and T. Rakpukdee. Comparative Study of Real-World Driving Cycles, Energy Consumption, and CO2 Emissions of Electric and Gasoline Motorcycles Driving in a Congested Urban Corridor. *Sustainable Cities and Society*, Vol. 45, 2019, pp. 619–627. https://doi.org/10.1016/j.scs.2018.12.031.
24. Kamble, S. H., T. V. Mathew, and G. K. Sharma. Development of Real-World Driving Cycle: Case Study of Pune, India. *Transportation Research Part D: Transport and Environment*, Vol. 14, No. 2, 2009, pp. 132–140. https://doi.org/10.1016/j.trd.2008.11.008.
25. Yang, Y., T. Li, H. Hu, T. Zhang, X. Cai, S. Chen, and F. Qiao. Development and Emissions Performance Analysis of Local Driving Cycle for Small-Sized Passenger Cars in Nanjing, China. *Atmospheric Pollution Research*, Vol. 10, No. 5, 2019, pp. 1514–1523. https://doi.org/10.1016/j.apr.2019.04.009.
26. Ho, S. H., Y. D. Wong, and V. W. C. Chang. Developing Singapore Driving Cycle for Passenger Cars to Estimate Fuel Consumption and Vehicular Emissions. *Atmospheric Environment*, Vol. 97, 2014, pp. 353–362. https://doi.org/10.1016/j.atmosenv.2014.08.042.
27. Cossalter, V. *Motorcycle Dynamics*, 2nd ed.Lulu.com, Morrisville, NC, 2006.
28. ABNT NBR 10312. *Veículos Rodoviários Automotores Leves - Determinação Da Resistência Ao Deslocamento Por Desaceleração Livre Em Pista de Rolamento e Simulação Em Dinamômetro*. Normas, 2019, pp. 1–17.
29. Ni, D., and D. Henclewood. Simple Engine Models for VII-Enabled in-Vehicle Applications. *IEEE Transactions on Vehicular Technology*, Vol. 57, No. 5, 2008, pp. 2695–2702. https://doi.org/10.1109/TVT.2008.917229.

30. Ben-Chaim, M., E. Shmerling, and A. Kuperman. Analytic Modeling of Vehicle Fuel Consumption. *Energies*, Vol. 6, No. 1, 2013, pp. 117–127. https://doi.org/10.3390/en6010117.
31. IBGE. *Frota de Veículos*. Cidadeapé, 2018.
32. Pernambuco. *Plano Diretor Cicloviário Da Região Metropolitana Do Recife*. Pernambuco, 2014.
33. FENABRAVE. *Resumo Mensal Dezembro de 2014*. ISSUU, 2014.
34. INMETRO. *Dados Do PBEV Solicitados Em 2019 Ao INMETRO Por Meio Da Lei Nº 12.527/11*. INMETRO.
35. Azevedo, J. A. H., D. R. Cassiano, B. B. Feitosa, M. L. M. De Oliveira, E. P. Lima, and B. V. Bertoncini. Influências Dos Modos de Operação Nas Emissões de Poluentes Provenientes de Veículos Flex Em Região Urbana. *Transportes*, Vol. 25, No. 2, 2017, p. 91. https://doi.org/10.14295/transportes.v25i 2.1304.
36. Roso, V. R., and M. E. S. Martins. Evaluation of a Real-World Driving Cycle and its Impacts on Fuel Consumption and Emissions. *SAE Technical Paper Series*, Vol. 1, 2016. https://doi.org/10.4271/2015-36-0195.